IEEE Access
Multidisciplinary | Rapid Review | Open Access Journal

Received January 19, 2019, accepted February 5, 2019, date of publication February 11, 2019, date of current version February 27, 2019.

Digital Object Identifier 10.1109/ACCESS.2019.2898550

Wideband Phase-Gradient Metasurface Antenna With Focused Beams

JIA-JUN LIANG[1,2], GUAN-LONG HUANG[1,3], (Senior Member, IEEE), JIA-NING ZHAO[4], ZHI-JIAN GAO[5], AND TAO YUAN[1,5]

[1]Guangdong Provincial Mobile Terminal Microwave and Millimeter-Wave Antenna Engineering Research Center, College of Information Engineering, Shenzhen University, Shenzhen 518060, China
[2]Key Laboratory of Optoelectronic Devices and Systems of Ministry of Education and Guangdong Province, College of Optoelectronic Engineering, Shenzhen University, Shenzhen 518060, China
[3]State Key Laboratory of Millimeter Waves, Nanjing 210069, China
[4]School of Electronic Science and Engineering, University of Electronic Science and Technology of China, Chengdu 610054, China
[5]ATR National Key Laboratory of Defense Technology, College of Information Engineering, Shenzhen University, Shenzhen 518060, China

Corresponding authors: Guan-Long Huang (guanlong.huang@szu.edu.cn) and Tao Yuan (yuantao@szu.edu.cn)

This work was supported in part by the National Natural Science Foundation of China under Grant 61801300, in part by the State Key Laboratory of Millimeter Waves under Grant K201932, and in part by the New Teacher Natural Science Research Project of Shenzhen University under Grant 2018078.

ABSTRACT A transmitting lens antenna with focused beams by employing four-layer phase-gradient metasurface (PGMS) is proposed. A wideband slot-coupled antenna is mounted close to the focal position of the PGMS acting as a feed. The electromagnetic wave radiated through the feed source is transformed to plane wave within a wide frequency covering from 9.4 to 10.6 GHz. The in-band measured gain is from 16.7 to 19.4 dBi and a 3-dB gain bandwidth of around 10% is achieved, which demonstrates that the proposed four-layer PGMS still has the ability to focus electromagnetic wave within a wide frequency band efficiently though its transmission phase range at some specific frequency bands does not meet 360°.

INDEX TERMS Wideband, transmitting, slot-coupled antenna, phase-gradient metasurface.

I. INTRODUCTION

With the increasing demands on high speed and large channel capacity in modern mobile communication systems, broadband and high gain antenna technologies have been developed rapidly, especially in the high-frequency band of the fifth generation mobile communication [1]–[7]. The waveguide antennas [8], [9], microstrip antenna arrays [10], [11] and three-dimensional (3-D) lens antennas [12], [13], are some of the most popular high gain antennas. For the waveguide-based antennas, they are bulky and not suitable for miniaturization and integration. The microstrip antenna arrays are ideal high gain antennas for miniaturization and integration, but they face the severe problem of dielectric losses as the operating frequency getting higher, and also not suitable for high power applications. Additionally, the 3-D lens antenna especially the dielectric spherical lens antenna, which can manipulate the non-plane electromagnetic wave to plane wave by changing the permittivity inside the dielectric, is indeed a good candidate for realizing high gain antenna. However, most of the 3-D dielectric spherical lens antennas have a large volume and also are hard to achieve system-level integration. Nowadays, researchers have found a simple and easy way to transform a 3-D spherical lens antenna into a 2-D planar lens antenna [14]–[20]. Planar lens antenna particularly the phase gradient metasurface (PGMS) lens antenna has attracted significant attention due to its merits of high gain, simple structure, and low profile [21], [22]. The PGMS is a novel metasurface which was presented by Yu *et al.* to prove the generalized Snell's law [23]. In [21], a high-gain X-band lens antenna is proposed based on the basic theory of phase gradient metasurface, which opens up a new path for the PGMS in microwave practical application. Thereafter, a single layer PGMS lens antenna is presented, which further reduces the thickness of the PGMS by using a single layer element-group [22]. At present, most of the reported PGMS antennas are operating in a narrow band with typical relative bandwidth less than 2% [21], [22]. In order to further expand its practical deployment, PGMS lens antenna with broadband characteristic has to be investigated.

To investigate the focusing characteristics of the PGMS under the conditions of broadband high transmission coefficient with in-band phase differences less than 360°,

The associate editor coordinating the review of this manuscript and approving it for publication was Chow-Yen-Desmond Sim.

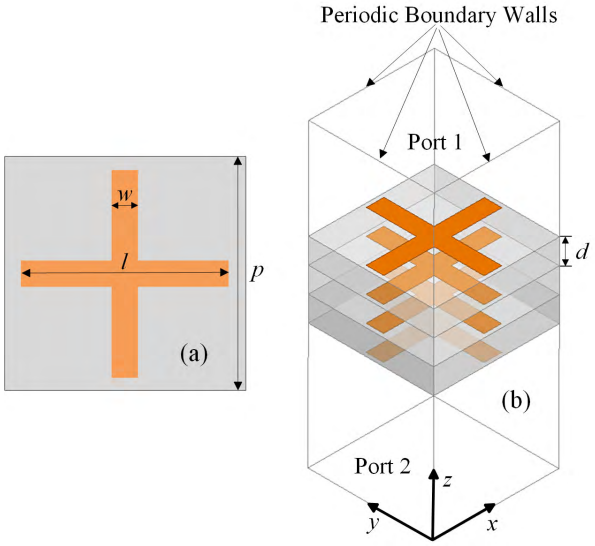

FIGURE 1. The proposed PGMS element and its simulated setup. (a) Top view. (b) Perspective view.

a broadband slot-coupled patch antenna acts as the feed source for the first time, which demonstrates that the proposed four-layer PGMS still has the ability to focus electromagnetic wave within a wide frequency band (9.4 GHz-10.6 GHz) efficiently, even if its transmission phase range only covers from 192° to 360°.

II. PGMS DESIGN

A. ELEMENT DESIGN

The basic structure of the proposed PGMS element is shown in Figure 1 with some key parameters indicated. It is made up of four-layer metallic planar structures and three intermediate dielectric layers. Each metallic layer contains a cross-type patch with a fixed width (w) and a variable length (l). The dielectric layer is a kind of F4B material with 2 mm thickness, relative dielectric constant of 2.2 and loss tangent of 0.017. The PGMS element is analyzed using ANSYS Electromagnetics Suite 17.2 by applying periodic boundaries in both x- and y- directions. In order to tune the phase variation efficiently, only the length of the cross-type patch (l) is adjusted and optimized while fixing $p = 10$ mm, $w = 1.62$ mm, and $d = 2$ mm.

Figure 2 exhibits the simulated transmission coefficients of the PGMS element against l at different frequencies. As can be seen from Figure 2(a), the $|S21|$ is greater than 0.72 across the frequency band of 9 GHz-10.6 GHz when l ranges from 6.24 mm to 8.64 mm, indicating a wideband and high transmission efficiency of the element in the X-band. The phase of S21 is shown in Figure. 2(b). A full transmission phase range of 360° is achieved at 10.2 GHz and 10.6 GHz while a wide transmission phase range of 271° is also obtained at 9.8 GHz; and the minimum transmission phase range of 192° is achieved at 9.4 GHz. In this case, it is possible to design a wideband PGMS lens antenna form 9.4 GHz-10.6 GHz with an elaborate design. Though the transmission phase range of

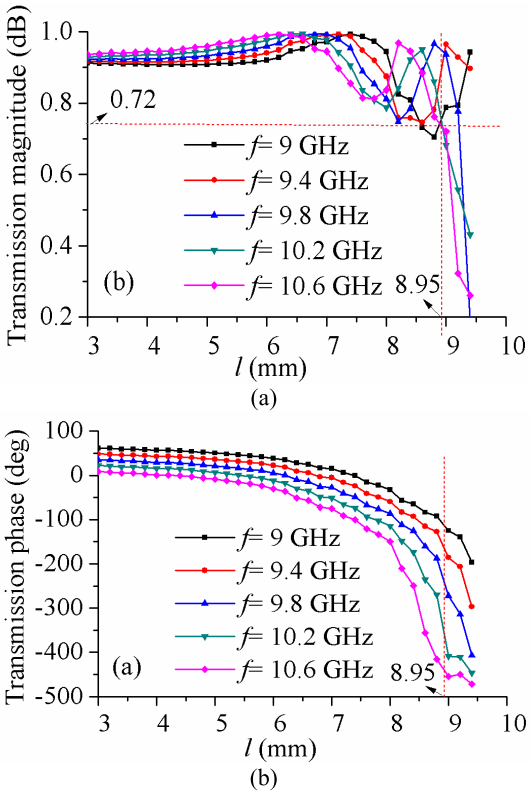

FIGURE 2. Simulated transmission coefficient of the PGMS element. (a) Magnitude. (b) Phase.

the element does not cover 360° below 10.2 GHz, where the maximum transmission phase variation is 215°, the element can be used for metasurface lens antenna with good performance, which has been verified by the former work [24].

B. PGMS DESING

The PGMS element would present some anomalous refraction when they form a supercell with a linearly varying phase gradient. The demonstration process can be found in [21] and [22]. In this paper, the supercell consists of eight elements. Each element has different length ln between 6.24 mm and 8.64 mm while the remaining parameters are kept unchanged, where the subscript n stands for the element number ($n = 1, 2, \ldots, 8$). To obtain a discrete phase shift with step of $\pi/4$ at 10.2 GHz, the corresponding lengths are $l_1 = 8.95$ mm, $l_2 = 8.83$ mm, $l_3 = 8.72$ mm, $l_4 = 8.58$ mm, $l_5 = 8.37$ mm, $l_6 = 8$ mm, $l_7 = 7.26$ mm, $l_8 = 6.24$ mm, respectively. To verify the supercell presents anomalous refraction, the relationship between the incidence wave and the refraction wave can be expressed in the following equation:

$$n_t \sin(\theta_t) - n_i \sin(\theta_i) = \frac{\lambda_0}{2\pi} \frac{d\varphi}{dx} \tag{1}$$

where φ is the phase discontinuity on the PGMS surface, n_t (n_i) is the refractive index of the refraction (incidence) medium while θ_t (θ_i) is the refractive (incidence) angle of the

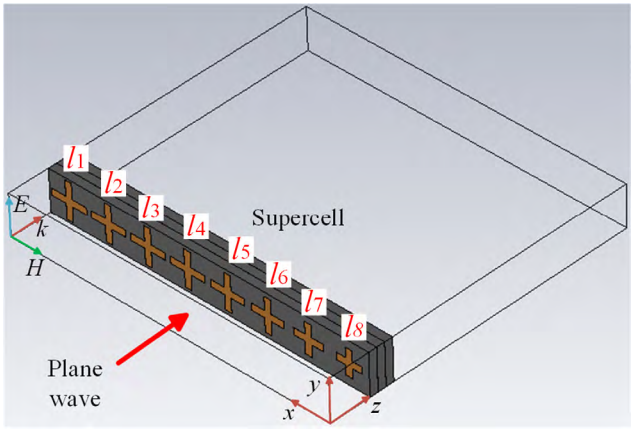

FIGURE 3. Simulated model of the supercell.

electromagnetic wave. With respect to a periodically installed supercell, $d\varphi dx = 2\pi/(np)$, where $n$represents the number of unit cells in the supercell. As the supercell is mounted in air (i.e., $n_t = n_i = 1$) and shined by normal incidence electromagnetic waves (i.e., $\theta_i = 0$ degree), θ_t is calculated by:

$$\theta_t = \sin^{-1}\left(\frac{\lambda_0}{2\pi} \times \frac{2\pi}{np}\right) \tag{2}$$

As shown in Figure 3, the supercell is excited by a plane wave with periodical boundaries in both x- and y- directions. According to (2), the theoretical deflecting angle θ_t at 9.4 GHz, 10 GHz, and 10.6 GHz are 23.51°, 22.02°, 20.67°, respectively, which are consistent with the simulated electric-field distribution shown in Figure 4.

It is obvious that, though the ranges transmission phase at 9.4 GHz and 10 GHz do not reached 360°, the electromagnetic deflection can still be obtained effectively. Subsequently, with the supercell's capability of manipulating electromagnetic wave being verified, to further achieve the planar transmitting lens, the refracted phase-difference distribution in the *xoy*-plane should obey the parabolic formulation given in (3):

$$\varphi(x, y) = \frac{2\pi}{\lambda}\left(\frac{x^2 + y^2}{4f}\right) + \varphi_1 \tag{3}$$

In equation (3), f represents the focal distance; $\varphi(x, y)$ is the refracted phase distribution on the planar transmitting lens (*xoy*-plane); φ_1 is the phase shift at the position $x = 0$, $y = 0$. Owing to the discrete phase generated only by the PGMS unit cells, the refracted phase-difference distribution on a metasurface lens is rewritten as:

$$\Delta\varphi(m, n) = \frac{2\pi}{\lambda_0}\left(\sqrt{(mp)^2 + (np)^2 + L^2} - L\right) \pm 2k\pi \quad (k = 0, 1, 2, \ldots) \tag{4}$$

In equation (4), $m(n)$ represents the unit cells in x (y)-direction; $\Delta\varphi(m, n)$ represents the phase-variation between the unit cells installed at the position of (m_p, n_p) and the one installed at the origin point ($m = 0, n = 0$). In order to complete the design of the PGMS, only seven different element patterns are employed to cover 360° phase variation in $+x$-direction. Hence, a PGMS with 13 × 13 unit cells is configured in this work. The element with $l_1 = 8.95$ mm is selected as the first cell ($m = 0, n = 0$) of the PGMS. The final transmission phase distribution plane diagram of the proposed PGMS is shown in Figure 5.

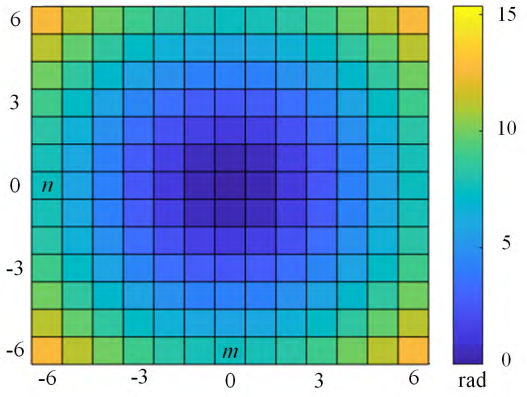

FIGURE 5. Phase distribution of the proposed PGMS.

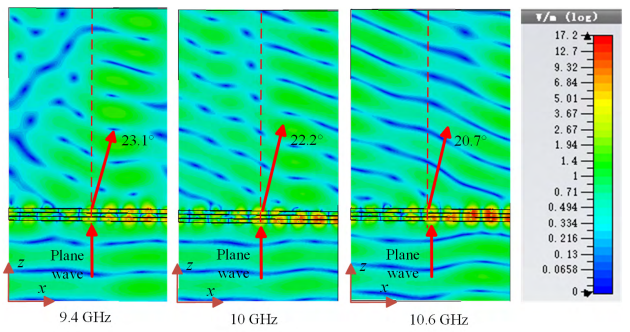

FIGURE 4. Simulated electric-filed distribution on *xoz*-plane.

III. WIDEBAND PGMS ANTENNA DESIGN AND TEST

In this paper, a slot-coupled patch antenna is proposed acting as the feed antenna for the wideband PGMS lens antenna, the structure of which is similar to the one in [25]. The configuration of the wideband antenna is shown in Figure. 6. The substrate used is Rogers RT/Duroid 5880 with a thickness of 0.787 mm, its relative dielectric constant and loss tangent are 2.2 and 0.002, respectively. A two-section matching microstrip line is used to excite the parasitic patch by a narrow slot opened in the metallic ground. The detailed parameters of the wideband antenna are given below: $W_1 = 2.3$ mm, $W_2 = 1$ mm, $W_p = 9.4$ mm, $W_s = 0.8$ mm, $L_s = 8$ mm, $L_{sub} = 25$ mm, $h = 0.787$ mm, $h_{gap} = 2.5$ mm.

The slot-coupled patch antenna and PGMS lens antenna are co-simulated by using CST Microwave Studio. To find the optimal focal position, the power density distribution map along the $+z$-axial direction at 10.2 GHz is analyzed first. As the peak power density appears at the position of about $z = 34$ mm, the location is selected as the position of the feed source. Then the slot-coupled patch antenna is placed

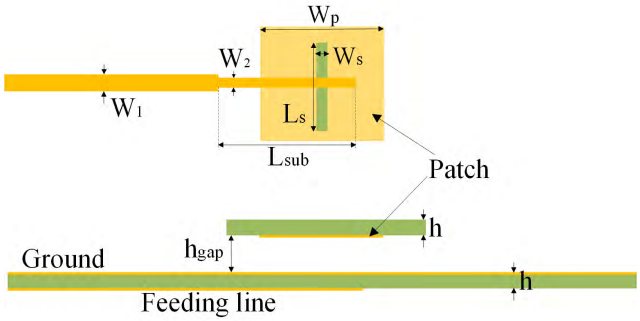

FIGURE 6. Structure of the wideband antenna.

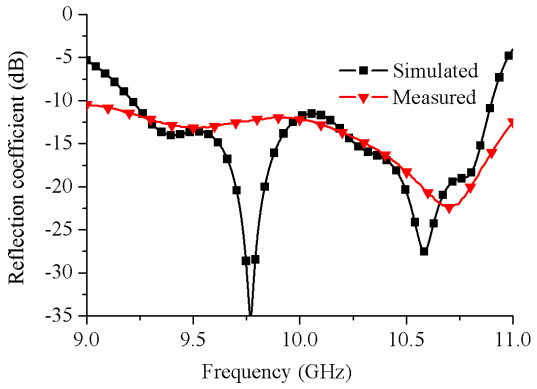

FIGURE 7. Simulated and measured reflection coefficients.

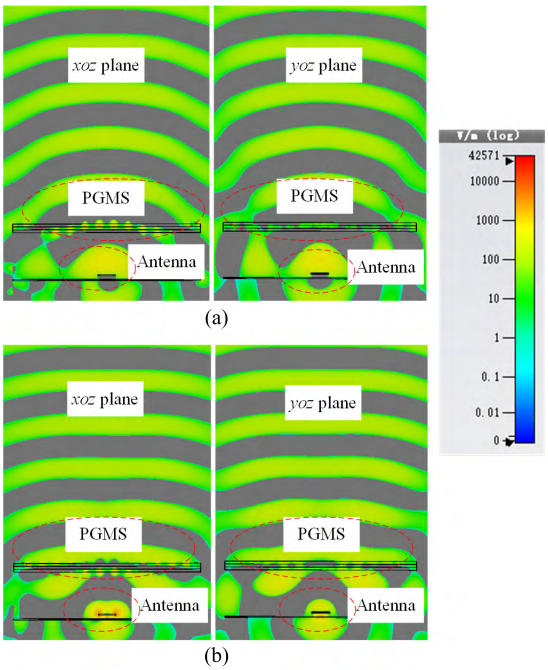

FIGURE 8. Simulated electric-field distributions *(Ex)* at: (a) 9.4 GHz; (b) 10.6 GHz.

34 mm away from the PGMS along $-z$-direction to feed the PGMS. The simulated and measured reflection coefficients of the slot-coupled patch antenna with and without PGMS

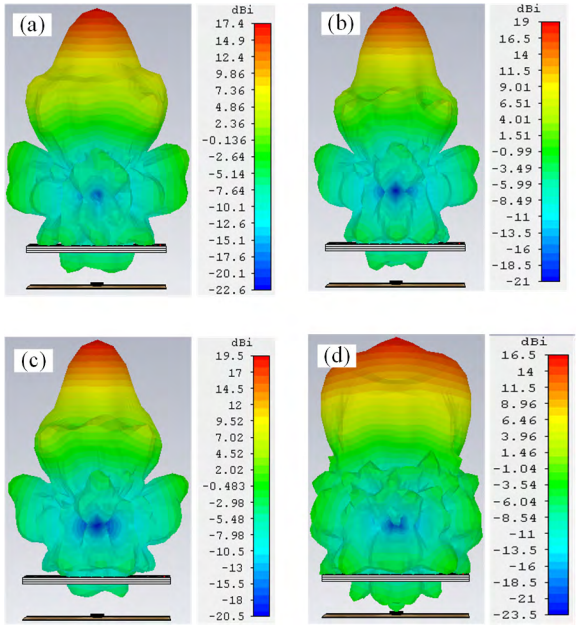

FIGURE 9. Simulated 3-D radiation patterns at: (a) 9.4 GHz; (b) 10 GHz; (c) 10.2 GHz; (d) 10.6 GHz.

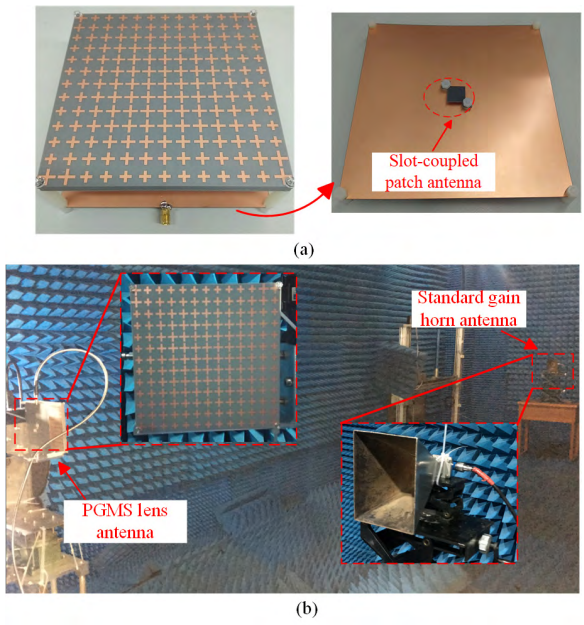

FIGURE 10. (a) Fabricated PGMS and slot-coupled patch antenna. (b) Measurement setup.

are plotted in Figure 7. The impedance bandwidth with $|S11| < -10$ dB is 9.2 GHz-10.8 GHz, which covers the transmission band (9.4 GHz-10.6 GHz) of the PGMS.

Figure 8 (a) and (b) show the simulated electric distribution (Ex) at 9.4 GHz and 10.6 GHz, respectively. As can be seen, the proposed PGMS transforms the quasi-spherical wave radiated by the slot-coupled patch antenna to approximate plane wave. The simulated 3-D radiation patterns at 9.4 GHz, 10 GHz, 10.2 GHz, and 10.6 GHz are also shown

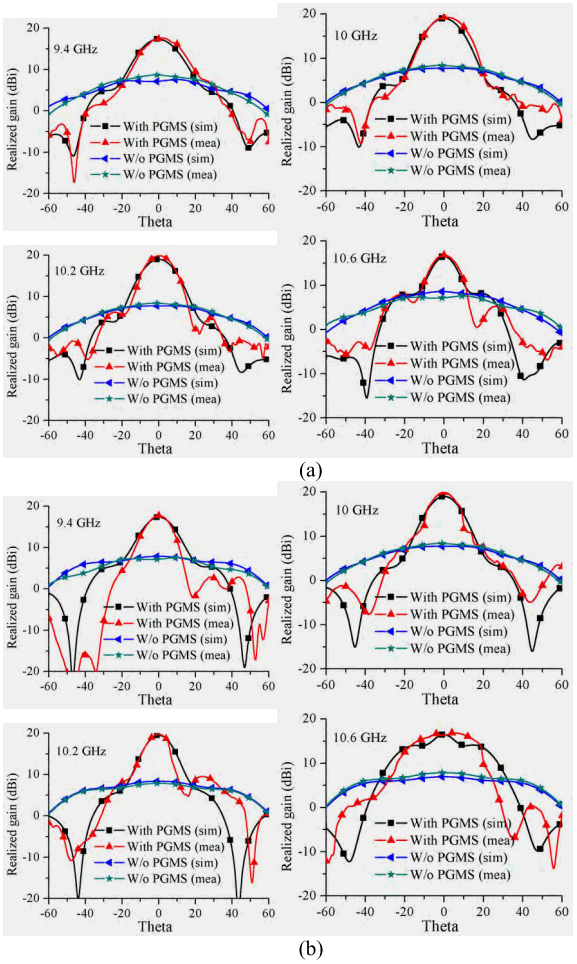

FIGURE 11. **Simulated and measured 2-D radiation patterns of the slotcoupled patch antenna with and without PGMS. (a) *xoz*-plane. (b) *yoz*-plane.**

in Figure 9. The maximum simulated gain of 19.5 dBi is obtained at 10.2 GHz while the minimum one is 16.5 dBi at 10.6 GHz.

Figure 10 shows the picture of the fabricated PGMS lens antenna and its measurement setup in the anechoic chamber. Figure 11 shows the simulated and measured 2-D gain radiation patterns of the slot-coupled wideband patch antenna with and without PGMS. As limited by the 2-D turntable using in the chamber during the test, the range of the elevation and azimuth angle only can cover from $-60°$ to $60°$. It can be seen that the maximum measured gain of the PGMS lens antenna increases about 11.3 dB compared with that of slot-coupled patch antenna alone at 10.2 GHz. Furthermore, the measured gains are consistent with the simulated ones. The maximum measured gain of 19.4 dBi is obtained at 10.2 GHz while the minimum one is 16.7 dBi at 10.6 GHz. The maximum aperture efficiency is about 37.8% at the center frequency. The 3-dB bandwidth of around 10% is achieved.

IV. CONCLUSION

A transmitting lens antenna with focused beams by employing four-layer phase-gradient metasurface is proposed. A broadband slot-coupled patch antenna is utilized as the feed source, which demonstrates that the proposed four-layer PGMS has the ability to focus electromagnetic wave within a wide frequency band (9.4 GHz-10.6 GHz) efficiently, though its transmission phase range only covers from 192° to 360°. The measured gains are consistent with the simulated ones; and the maximum measured gain is 19.4 dBi at 10.2 GHz while the minimum one is 16.7 dBi at 10.6 GHz with the 3-dB gain bandwidth of around 10%.

REFERENCES

[1] T. Li, F.-S. Zhang, F. Zhang, Y.-L. Yao, and J. Zhang, "Wideband and high-gain uniform circular array with calibration element for smart antenna application," *IEEE Antennas Wireless Propag. Lett.*, vol. 15, pp. 230–233, Feb. 2015.

[2] F. H. Lin and Z. N. Chen, "Low-profile wideband metasurface antennas using characteristic mode analysis," *IEEE Trans. Antennas Propag.*, vol. 65, no. 4, pp. 1706–1713, Apr. 2017.

[3] P.-Y. Qin, L.-Y. Ji, S.-L. Chen, and Y. J. Guo, "Dual-polarized wideband fabry-perot antenna with quad-layer partially reflective surface," *IEEE Antennas Wireless Propag. Lett.*, vol. 17, no. 4, pp. 551–554, Apr. 2018.

[4] J. Zhu, S. Liao, S. Li, and Q. Xue, "60 GHz wideband high-gain circularly polarized antenna array with substrate integrated cavity excitation," *IEEE Antennas Wireless Propag. Lett.*, vol. 17, no. 5, pp. 751–755, May 2018.

[5] F. H. Lin and Z. N. Chen, "Truncated impedance sheet model for low-profile broadband nonresonant-cell metasurface antennas using characteristic mode analysis," *IEEE Trans. Antennas Propag.*, vol. 66, no. 10, pp. 5043–5051, Oct. 2018.

[6] J. Zhao *et al.*, "A compact ka-band monopulse cassegrain antenna based on reflectarray elements," *IEEE Antennas Wireless Propag. Lett.*, vol. 17, no. 2, pp. 193–196, Feb. 2018.

[7] F. H. Lin and Z. N. Chen, "A method of suppressing higher order modes for improving radiation performance of metasurface multiport antennas using characteristic mode analysis," *IEEE Trans. Antennas Propag.*, vol. 66, no. 4, pp. 1894–1902, Apr. 2018.

[8] Z. Shen and C. Feng, "A new dual-polarized broadband horn antenna," *IEEE Antennas Wireless Propag. Lett.*, vol. 4, no. , pp. 270–273, Aug. 2005.

[9] M. K. T. Al-Nuaimi, W. Hong, and Y. Zhang, "Design of high-directivity compact-size conical horn lens antenna," *IEEE Antennas Wireless Propag. Lett.*, vol. 13, pp. 467–470, 2014.

[10] S.-W. Qu, D.-J. He, S.-W. Yang, and Z.-P. Nie, "Novel parasitic micro strip arrays for low-cost active phased array applications," *IEEE Trans. Antennas Propag.*, vol. 62, no. 4, pp. 1731–1737, Apr. 2014.

[11] Y. Li, Z. Zhang, C. Deng, Z. Feng, and M. F. Iskander, "2-D planar scalable dual-polarized series-fed slot antenna array using single substrate," *IEEE Trans. Antennas Propag.*, vol. 62, no. 4, pp. 2280–2283, Apr. 2014.

[12] H. F. Ma, B. G. Cai, T. X. Zhang, Y. Yang, W. X. Jiang, and T. J. Cui, "Three-dimensional gradient-index materials and their applications in microwave lens antennas," *IEEE Trans. Antennas Propag.*, vol. 61, no. 5, pp. 2561–2569, May 2013.

[13] M. Liang, W. R. Ng, K. Chang, K. Gbele, M. E. Gehm, and H. Xin, "A 3-D Luneburg lens antenna fabricated by polymer jetting rapid prototyping," *IEEE Trans. Antennas Propag.*, vol. 62, no. 4, pp. 1799–1807, Apr. 2014.

[14] S. Sun, Q. He, S. Xiao, Q. Xu, Z. Li, and L. Zhou,"Gradient-index metasurfaces as a bridge linking propagating waves and surface waves," *Nature Mater.*, vol. 11, pp. 426–431, Apr. 2012.

[15] S. Sun *et al.*, "High-efficiency broadband anomalous reflection by gradient meta-surfaces," *Nano Lett.*, vol. 12, no. 12, pp. 6223–6229, 2012.

[16] M. Pu *et al.*, "Broadband anomalous reflection based on gradient low-Q meta-surface," *AIP Adv.*, vol. 3, 2013, Art. no. 052136.

[17] K. Song, J. Kim, S. Hur, J.-H. Kwak, S.-H. Lee, and T. Kim, "Directional reflective surface formed via gradient-impeding acoustic meta-surfaces," *Sci. Rep.*, vol. 6, p. 32300, Aug. 2016.

[18] T. Cai, G.-M. Wang, X.-L. Fu, J.-G. Liang, and Y.-Q. Zhuang, "High-efficiency metasurface with polarization-dependent transmission and reflection properties for both reflectarray and transmitarray," *IEEE Trans. Antennas Propag.*, vol. 66, no. 6, pp. 3219–3224, Jun. 2018.
[19] R. Y. Wu, Y. B. Li, W. Wu, C. B. Shi, and T. J. Cui, "High-gain dual-band transmitarray," *IEEE Trans. Antennas Propag.*, vol. 65, no. 7, pp. 3481–3488, Jul. 2017.
[20] C. Pfeiffer and A. Grbic, "Planar lens antennas of subwavelength thickness: Collimating leaky-waves with metasurfaces," *IEEE Trans. Antennas Propag.*, vol. 63, no. 7, pp. 3248–3253, Jul. 2015.
[21] H. Li, G. Wang, H.-X. Xu, T. Cai, and J. Liang, "X-band phase-gradient metasurface for high-gain lens antenna application," *IEEE Trans. Antennas Propag.*, vol. 63, no. 11, pp. 5144–5149, Nov. 2015.
[22] H. Li, G. Wang, J. Liang, X. Gao, H. Hou, and X. Jia, "Single-layer focusing gradient metasurface for ultrathin planar lens antenna application," *IEEE Trans. Antennas Propag.*, vol. 65, no. 3, pp. 1452–1457, Mar. 2017.
[23] N. Yu *et al.*, "Light propagation with phase discontinuities: Generalized laws of reflection and refraction," *Science*, vol. 334, no. 6054, pp. 333–337, Oct. 2011.
[24] T. Li and Z. N. Chen, "Miniaturized metasurface unit cell for microwave metalens antennas," in *Proc. Int. Conf. Electromagn. Adv. Appl. (ICEAA)*, Sep. 2017, pp. 980–983.
[25] N. Wang, L. Talbi, Q. Zeng, and J. Xu, "Wideband Fabry-P'erot resonator antenna with electrically thin dielectric superstrates," *IEEE Access.*, vol. 4, pp. 14966–14973, Apr. 2018.

JIA-JUN LIANG received the B.E. degree in electronic science and technique from the Guilin University of Electronic Technology, Guilin, China, in 2012, the M.E. degree in radio physics from the University of Electronic Science and Technology of China, Chengdu, China, in 2015, and the Ph.D. degree from the College of Information Engineering, Shenzhen University, Shenzhen, Guangdong, China, in 2018, where he is currently a Postdoctoral Research Fellow with the College of Information Engineering. He has been with the Department of Physics, The Hong Kong University of Science and Technology, as a Research Assistant, from 2016 to 2017. His current research interests include 3-D printed antennas, liquid antennas, RF front-end devices, wireless communication, and radar systems.

GUAN-LONG HUANG (M'11–SM'18) received the B.E. degree in electronic information engineering from the Harbin Institute of Technology, Harbin, China, and the Ph.D. degree in electrical and computer engineering from the National University of Singapore, Singapore.

He is currently an Assistant Professor with the College of Information Engineering, Shenzhen University, Shenzhen, Guangdong, China. He also serves as the Deputy Director of the Guangdong Provincial Mobile Terminal Microwave and Millimeter-Wave Antenna Engineering Research Center. Prior to joining the university, he has been with the Temasek Laboratories, National University of Singapore, as a Research Scientist, and the Nokia Solutions and Networks System Technology as a Senior Antenna Specialist, from 2011 to 2017. He has authored or co-authored more than 100 papers in journals and conferences. His research interests include the design and implementation of planar antenna arrays, 5G base-station and mobile RF front-end devices/antennas, phased antenna arrays, channel coding for massive MIMO applications, and 3-D printing technology in microwave applications. He is currently serving as an Associate Editor for the journal IEEE Access.

JIA-NING ZHAO received the B.Sc. degree from the School of Information and Communication, Guilin University of Electronic Technology, Guilin, China, in 2013. He is currently pursuing the Ph.D. degree with the School of Electronic Science and Engineering, University of Electronic Science and Technology of China, Chengdu, China. His research interests include transmitarray, reflectarray antenna design, reflector antenna design, and novel control the mode based on the transmitarray surface.

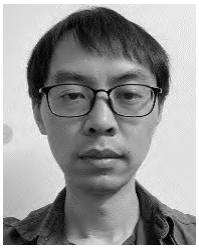

ZHI-JIAN GAO received the master's degree from Shenzhen University, Shenzhen, China, where he is currently an Experimental Engineer with the ATR National Key Laboratory of Defense Technology. His current research interests include wireless sensor networks and microwave communication.

TAO YUAN received the bachelor's and master's degrees from Xidian University, China, and the Ph.D. degree from the National University of Singapore, Singapore. He is currently a Professor with the College of Information Science, Shenzhen University. His current research interests include developing novel RF modules and antennas for mobile terminal and 5G applications.